T. Tomita, C. E. Sjøgren, P. Klæboe, G. N. Papatheodorou and E. Rytter, High Temperature Infrared and Raman Spectra of Aluminium Chloride Dimer and Monomer on the Vapour Phase. J....

ARTICLE *in* JOURNAL OF RAMAN SPECTROSCOPY · JANUARY 1983

Impact Factor: 2.67

High-Temperature Infrared and Raman Spectra of Aluminium Chloride Dimer and Monomer in the Vapour Phase

T. Tomita,* C. E. Sjøgren and P. Klaeboe†
Department of Chemistry, University of Oslo, Oslo 3, Norway

G. N. Papatheodorou
Department of Chemical Engineering, University of Patras, Patras, Greece

E. Rytter
Institute of Inorganic Chemistry, University of Trondheim, N-7034 Trondheim-NTH, Norway

The infrared spectra of aluminium chloride vapour (Al_2Cl_6 and $AlCl_3$) including $Al_2^{35}Cl_6$ and $Al_2^{37}Cl_6$ at 473–843 K were measured in the region 700–50 cm^{-1} with an evacuable Fourier transform spectrometer by transmission and emission techniques. Evacuable cells of nickel were employed having windows of type IIa diamond and sealed with gold O-rings. Raman spectra of Al_2Cl_6 vapour at *ca* 500 K and of $AlCl_3$ at 1075 K with pressures from 0.3 to 10 atm were recorded, polarization measurements were carried out and additional spectra of the ^{35}Cl and ^{37}Cl compounds were obtained. The dimer spectra were interpreted in terms of D_{2h} symmetry. All the nine Raman-active and seven of the infrared-active dimer fundamentals were assigned. The IR active mode $\nu_{10}(B_{1u})$, expected below 40 cm^{-1}, and the inactive mode $\nu_5(A_u)$ were left unassigned. The monomer spectra were interpreted in terms of D_{3h} symmetry and all four fundamentals were assigned. A dimer force field, involving 12 independent force constants, was derived. The calculated frequencies were fitted with a least-squares programme to 30 observed fundamentals of $Al_2^{35}Cl_6$ and $Al_2^{37}Cl_6$ and 14 additional isotopic shifts transferred from previous matrix isolation spectra. A complete force field for the monomer was derived, using the four observed fundamentals and seven isotopic shifts transferred from previously reported matrix isolation spectra.

INTRODUCTION

The molecular structures of aluminium chloride vapour as a dimer and monomer have been studied by various methods, including electron diffraction,[1,2] Raman[3–5] and infrared[6] spectroscopy. The dimer molecules (Al_2Cl_6) undoubtedly have D_{2h} structure in the vapour phase and in the melt. Also, it now seems well established that in the vapour phase the monomers ($AlCl_3$) have D_{3h} symmetry.[2,7]

In the earlier Raman spectroscopic studies of Al_2Cl_6 as a melt[8–10] and vapour,[3–5] eight of the nine Raman-active modes of Al_2Cl_6 were tentatively assigned. However, the infrared spectra of this compound as a melt or as a vapour are experimentally difficult to obtain since very few window materials are suitable. Thus, the windows should be (a) transparent to the region of interest (1000–30 cm^{-1}), (b) able to withstand high temperatures (around 700 °C) and (c) chemically inert towards the corrosive melts or vapours.

In a pioneering study, Klemperer[6] avoided some of these restrictions. Using KBr windows protected by a cold gas curtain he obtained an infrared emission spectrum and observed the three highest fundamentals situated above 400 cm^{-1}. All the additional infrared studies[7,11–13] and certain Raman investigations[7,13] were based on the matrix isolation technique. In these investigations the Al_2Cl_6 (or $AlCl_3$) was quenched in an inert argon or nitrogen matrix and observed at 10–20 K. From these studies eight of the nine Raman-active modes and seven of the eight infrared-active fundamentals were assigned. In addition, fundamentals of monomeric $AlCl_3$ were recorded in the Raman spectra of the vapour above 800 °C[3,5] or by quenching the superheated vapour in an argon matrix.[7,11]

The advantages of the matrix isolation technique are well known, particularly the narrow band widths which permit isotopic shifts to be determined accurately. However, the technique also has disadvantages compared with the direct studies of the vapour. Thus, additional bands caused by site effects in the matrices are commonly observed. Also, the observed bands are frequently considerably shifted from the vapour phase values, making force constant calculations less reliable.

We have recently constructed[14] infrared cells fitted with type IIa diamond windows, which are suitable for the study of corrosive vapours up to 600 °C under isothermal conditions. One of the cells was designed for transmission studies of vapours and the other cell can be used for emission studies of vapours or melts. They were both employed in combination with an evacuable fast-scan Fourier transform spectrometer. So far these cells have been used to study infrared transmission and emission spectra of various Group IIIb

* Present address: Mitsubishi Light Metal Industries Ltd, 1000 Kamoshida Midori-ku, Yokohama, Japan.
† Author to whom correspondence should be addressed.

CCC-0377-0486/83/0014-0415 $05.50

halide vapours[15] and emission spectra of various chloroaluminate melts.[16] Unlike the matrix isolation cryostats, our isothermal cells are suitable for studying monomer–dimer equilibria or complex formation reversibly as a function of temperature.

Some of our preliminary infrared results of the dimers Al_2Cl_6, Al_2I_6 and Ga_2Cl_6 and the monomers AlI_3 and $GaCl_3$ observed in the vapours have been reported.[15,17] In this paper we report the detailed Raman and infrared spectra of Al_2Cl_6 and $AlCl_3$ observed in the temperature range 473–1075 K. Finally, the spectroscopic data from the vapour were used to derive force fields for the aluminium chloride monomer and dimer.

EXPERIMENTAL

Raman

Raman spectra of the aluminium chloride vapours were obtained by methods described in more detail elsewhere.[18,19] Evacuated and sealed fused silica cells containing the solid salt were placed in a resistance heated furnace and the vapour spectra were excited with an Ar^+(~15 W all lines) or a Kr^+ (~400 mW all lines) CW laser. The scattered radiation was dispersed with a SPEX 1400 double monochromator and detected with a photomultiplier tube using Photon-counting techniques.

The Raman (optical) cells containing the salt vapours with pressures less than 5 atm were made of fused silica tubing (20 mm o.d., 18 mm i.d. and 2.5–5 cm long). For vapours having a pressure above 5 atm, a silica tubing with 3 mm wall thickness was used. Pre-weighed amounts of the chemicals were transferred into a dry and degassed cell of known volume V. The cell was sealed under vacuum and attached to a fused silica manipulation rod. The 'ideal gas' pressure, P_0, of Al_2Cl_6 at a temperature T was calculated from the amount of Al_2Cl_6 in the Raman cell.

Five different cells were made having P_0 pressures of (i) ~0.3, (ii) ~0.6, (iii) ~1.0, (iv) ~2.0 and (v) ~10 atm at 500 K. Owing to the dissociation, the pressure of the dimer, P', and monomer, P_1, are related to the equilibrium constant, k, and the pressure of the added Al_2Cl_6, P_0, through the relationships

$$Al_2Cl_6 = 2AlCl_3 \tag{1}$$

$$P' = P_0 + k/8\left[1 - \left(\frac{16P_0}{k} + 1\right)^{1/2}\right] \tag{2}$$

$$P_1 = (kP')^{1/2} \tag{3}$$

Four cells having isotopically substituted aluminium chlorides ($Al^{35}Cl_3$, $Al^{37}Cl_3$) with pressures $P_0 \approx 0.5$ atm were also made. The isotopically substituted salts were prepared *in situ* in the Raman cell by heating together pure Al wire and $^{37}Cl_2$ or $^{35}Cl_2$ gas of known pressure. The isotopes of the chlorine gas were produced from high purity $Na^{37}Cl$ and $Na^{35}Cl$. Equations (2) and (3) suggest that the Raman spectrum of the $AlCl_3$ monomer can be best obtained from low P_0 pressure cells at elevated temperatures (800 K). It was found that attack of aluminium chloride on the silica cells was proportional to the ratio P_1/P'. For example, a cell having $P_0 \approx 10$ atm could be heated to 700 K overnight with no detection of attack (no cloudiness) on the silica cell whereas a cell having $P_0 \approx 0.2$ atm was 'clouded' easily within 1 h at ~650 K.

Infrared

The aluminium chloride used in the infrared study was prepared by reaction between HCl and aluminium chips (99.998% pure from Vigeland Brug, Norway) at 720 K. The product was purified by subsequent sublimation on a vacuum line and 1–4 mg samples were sealed in silica tubes. The ampoules were opened and a determined quantity placed in the transmission or emission cells in the dry air atmosphere of a glove-box.

The transmission and emission cells used in this investigation have been described previously,[14,16] but the main principles will be reported here.

The multipurpose cell system used for emission or transmission consists of a steel cylinder with exchangeable inner parts selected for the actual experiment. The design provides a good alignment of the sample container and an even pressure on the diamond window, reducing the risk of breaking it. The correct position of the window is controlled through the viewing slits.

For emission work, the solid sample is filled into a nickel crucible. The outer lower part of the crucible is polished and acts as a reflecting backplate, thus reducing black-body radiation. For the same reason, the support for the window is gold-plated. The window itself is 1 mm thick with a diameter of 8 mm. It is made of type IIa diamond (D. Drukker & Zn., Holland) and sealed to a nickel container by a gold O-ring produced by welding a 0.5 mm diameter wire. In most of the experiments, the sample thickness was controlled with a spacer made from the same gold wire. However, path lengths larger than 0.5 mm can easily be used in the vapour studies. Removal of the spacer results in a cell excellent for emission spectroscopy of liquids and molten salts for which a sample thickness of *ca* 0.01 mm is preferable. The sample container of the transmission cell consisted of two nickel halves which were plasma welded together. It has a gas volume of 2.3 cm^3, a path length of 40 mm and is closed with two 6.4 mm diameter diamond windows of 1 mm thickness.

The 6.4 mm diameter windows were also used in the special absorption cell illustrated in Fig. 1. This cell was constructed in order to increase the cell volume to 9.9 cm^3. Further, the thermal expansion of the materials employed were matched to give a slightly heavier pressure on the windows at higher temperatures.

Before each experiment the emission or transmission cells were placed in a tube of silica and baked at *ca* 800 K and *ca* 10^{-2} Torr overnight to remove adsorbed moisture. The cell and the silica tube were cooled to ambient temperature and, while still evacuated, brought into the dry-box. Here the silica tube was opened and the cell was filled with the pre-weighed amount of sample. As the next step the absorption cell (Fig. 1) was evacuated in a specially designed vacuum desiccator (Fig. 2) placed inside the dry-box. After a pressure of *ca* 10^{-3} Torr was reached the cell was closed by turning the steel bolts (7) by mechanical connectors extending

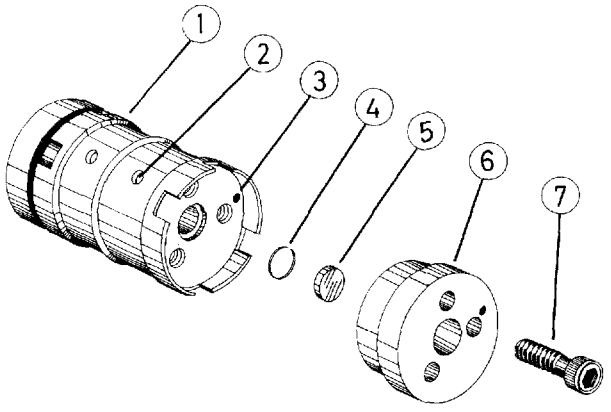

Figure 1. Transmission cell: (1) nickel cell body; (2) hole for positioning the cell in the vacuum desiccator; (3) thermocouple well; (4) gold gasket; (5) diamond window; (6) stainless-steel cover; (7) mild steel bolts.

through the desiccator lid. The emission cell, when used both for vapour and melt studies, was also evacuated in a unit similar to that shown in Fig. 2. The cell was placed in a steel furnace with heating elements of 0.5 mm Kanthal wire on a silica tube, insulated with ceramic fibres and a water-cooled jacket. The temperatures were measured by chromel–alumel thermocouples.

The transmission cell was placed in a furnace inside a separately evacuable unit (Fig. 3) fitted to the sample compartment of the evacuable Bruker Fourier transform spectrometer. This unit was fitted with demountable windows of polyethylene or KBr, to avoid contamination of the spectrometer with corrosive vapours in cases of leaks. However, since no serious leaks ever developed, the windows were removed to increase the optical throughput, making the unit an integral part of the evacuable spectrometer. The absorption cell was

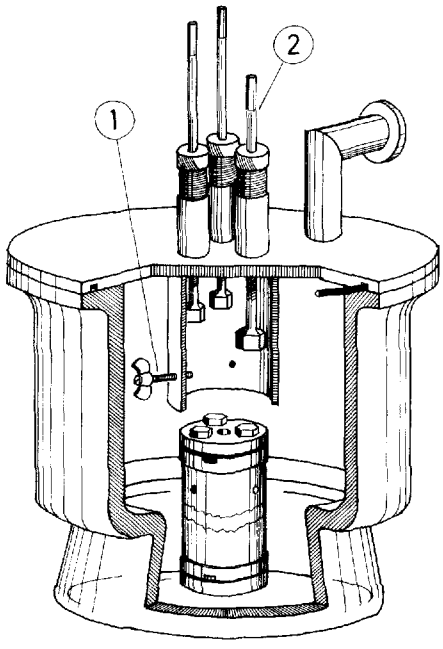

Figure 2. Vacuum desiccator: (1) bolt for positioning of the cell; (2) vacuum tight mechanical connectors for tightening the cell bolts.

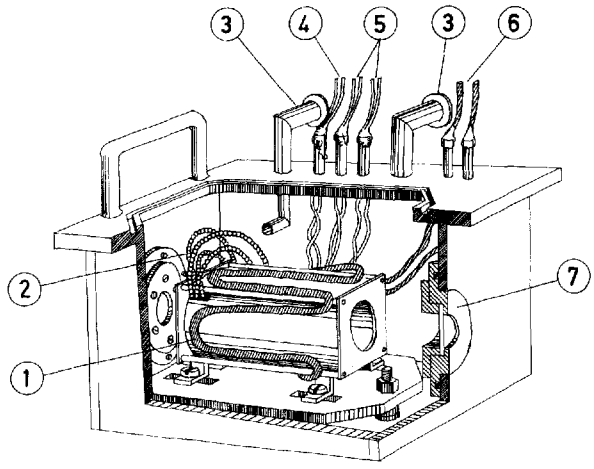

Figure 3. Furnace assembly: (1) water-cooled jacket; (2) electrical wires; (3) vacuum flange; (4) thermocouple connectors; (5) external furnace connectors; (6) water hose; (7) removable window.

carefully centred at the focal point of the sample compartment. With two diamond windows of 6.4 mm diameter, *ca* 10% of the radiation was transmitted through the empty cell. At temperatures above 700 K a background signal of light emitted from the sample, modulated in the spectrometer and retransmitted through the cell, may distort the spectrum. This effect could be avoided (or reduced) by slightly defocussing the image on the beam splitter, an advantage inherent in the optical design of this spectrometer.

The emission cell and the appropriate furnace was mounted vertically on the optical bench of the source compartment. A demountable mirror, fitted with micrometer adjustments placed in front of the source, directed the radiation into the spectrometer (see Fig. 3 in Ref. 14). When the mirror was removed the spectrometer could be used for general-purpose transmission studies. The modular design of the spectrometer allowed removal of the sample compartment during emission work, thus removing reflection losses from four mirrors. In addition, the optical path length was reduced to *ca* 1 m.

All the spectra were recorded with a Bruker Model 114 C fast-scan Fourier transform spectrometer evacuable to *ca* 0.1 Torr. Most of the spectra were recorded between 700 and 50 cm^{-1}, using Mylar beam splitters of thickness 3.5, 6, 12 and 23 μm and a standard TGS detector. The spectra were recorded with 4 or 8 cm^{-1} resolution and 500 or 1000 scans were collected.

A cylindrical cavity covered with carbon black functioned as a black-body reference in the emission work. The transmission spectra were ratioed against the spectra of an empty cell recorded at the same temperature.

RESULTS AND DISCUSSION

Raman spectra

At temperatures near the sublimation point (~450 K) of aluminium chloride the dimeric Al_2Cl_6 is the predominant vapour species. Figure 4 shows the Raman

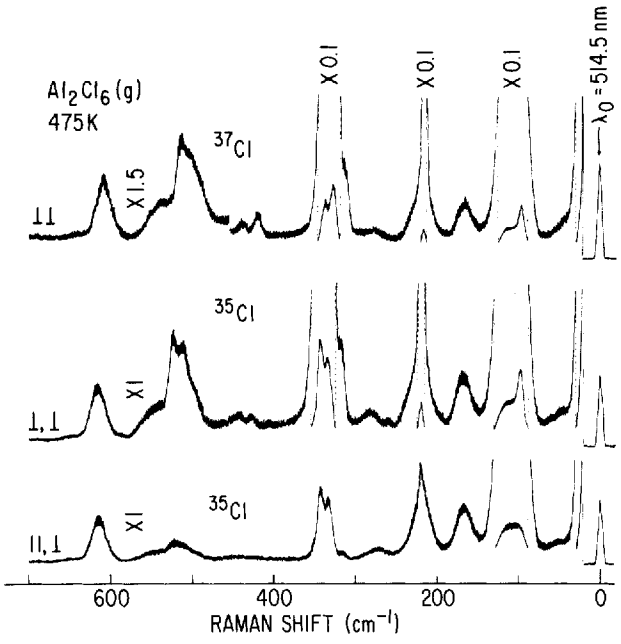

Figure 4. Raman spectra of isotopically substituted aluminium chloride vapours at 475 K. Spectral slit width, 6 cm^{-1}; λ_0 = 514.5 nm; laser power, 5 W; time constant, 0.25 s. Note that the intensities of the Fermi resonance doublet at ~340 cm^{-1} change with isotopic substitution.

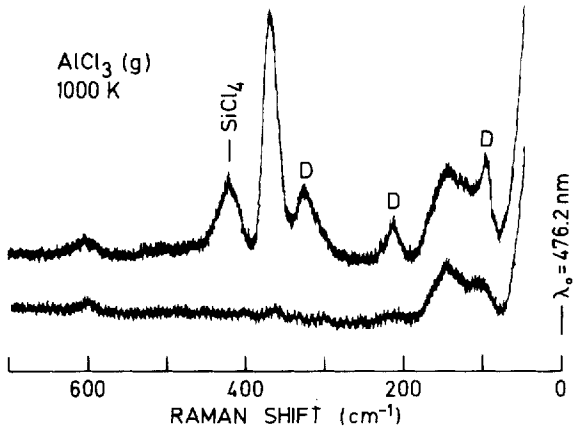

Figure 5. Raman spectrum of aluminium chloride monomer at 1000 K (D denotes dimer band).

spectra of the isotopically substituted ^{37}Cl and ^{35}Cl aluminium chloride vapours at 475 K. The calculated pressure P_0 in these cells was approximately 0.5 atm. Raman spectra using aluminium trichloride with natural chlorine were also recorded from all cells listed in the experimental section. In Table 1 the frequencies of the occurring bands, their relative intensities and depolarization ratios at 500 K are listed for the 'natural' salt. A comparison of our results with those of the earlier authors[3–5] is given in the table. A number of additional bands were observed and, as reported previously,[5] the band at ~335 cm^{-1} is a polarized doublet. Increasing the temperature decreases the intensities of all the dimer bands listed in Table 1 and gives rise to new bands which are due to the $AlCl_3$ monomer (see Table 3 and Fig. 5).

The effect of temperature T and pressure P_0 on the Raman intensities of the $AlCl_3$ relative to the Al_2Cl_6 intensities was found to be as expected from Eqn (2). This is shown in Fig. 6, where the ν_1 fundamental of $AlCl_3$ increases its intensity relative to the 330 cm^{-1} band of Al_2Cl_6 with decreasing P_0 and/or increasing temperature.

Measurements of the Raman spectra of the pure isotopic species $Al_2^{35}Cl_6$ and $Al^{37}Cl_6$ obtained under similar conditions (of pressure and temperature) gave the wavenumbers for $Al_2^{35}Cl_6$ and the shifts $\nu^{35}_{Cl} - \nu^{37}_{Cl}$ listed in Table 2. Similar shifts reported by Rohrbasser[5] are also included.

Table 1. Raman spectral data for aluminium chloride dimer (Al_2Cl_6)

Vapour						Melt: this work (475 K)			Matrix isolation				
This work (500 K)			Ref. 4	Ref. 3	Ref. 5				Ref. 7	Ref. 13			
Freq.	Rel. int.	Dep. ratio	(623 K): freq.	(500 K): freq.	(523 K): freq.	Freq.	Rel. int.	Dep. ratio	freq. (Ar)	Freq. (Ar)	Freq. (N_2)	Interpretation	
650	1	0.0										$\nu_8+\nu_{10}$	A_g
613	10	0.81	608	612 D	608 m D	610	15	0.78	613	612	604	ν_{11}	B_{2g}
547	6 (sh)	>0.7										$\nu_{13}+\nu_{18}$	B_{1g}
522	12	0.0											
510	12	0.0	501		501 m P	512	30	0.15	523	523	520	ν_1	A_g
495	2 (sh)	0.0										$\nu_{11}-\nu_{12}$	A_g
440	2	0.0	438		440 w D	440	5	0.0				$\nu_6+\nu_7$	A_g
352	12 (sh)	0.0	385									$2\nu_9$	A_g
341	170	0.01	336	336 P	339 s P	341	375	0.01	342	342	347	ν_2[a]	A_g
331	165	0.01			329 s P							$2\nu_7$[a]	A_g
316	12 (sh)	0.0			315 w D							$\nu_3+\nu_4$	A_g
280	6	0.55	285		280 w D	290	20	0.0	283	284	289	$\nu_6 B_{1g}, 2\nu_{18}$	A_g
218	100	0.12	217	217 P	217 s P	218	100	0.27	219	219	221	ν_3	A_g
167	12	0.87	168	165	166 m D	166	35	0.75	166	166	162	ν_7	B_{1g}
114	95	0.85	115	117 P	112 s D	118	125	0.97	122	121	122	ν_{12}	B_{2g}
97	200	0.40		99 P	95 s P	102	140	0.76	107	106.5	107	ν_4	A_g
				77 D					77				
48	6	P										$2\nu_{10}$	A_g

[a] Presumably Fermi resonance, see text.

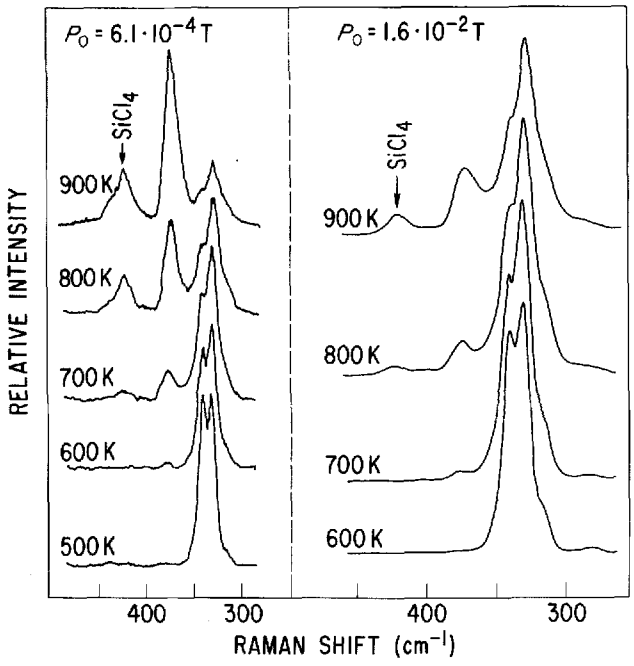

Figure 6. Portions of Raman spectra of aluminium chloride dimer and monomer at different temperaures and pressures. Spectral slit width, 6 cm^{-1}; $\lambda_0 = 488.0$ nm; laser power, 500 mW; time constant, 1 s.

Various temperature- and pressure-dependent changes of the relative intensities of the Al_2Cl_6 bands were observed. The following were found relative to the intensity of the band at 218 cm^{-1}. (*i*) The intensity of the band at 340 cm^{-1} increases (relative also to the band at 331 cm^{-1}) with decreasing temperature and/or increasing pressure. The temperature effect is well pronounced while the pressure effect can be clearly seen only after the bands in the 300 to 350 cm^{-1} region are resolved into Gaussians. (*ii*) The intensity of the band at 522 cm^{-1} increases with decreasing temperature. Increasing pressure appears to increase the intensity of this band slightly but, owing to the weak Raman signal in this region, the pressure effect is not conclusive. (*iii*) Increasing pressure or decreasing temperature slightly decreases the intensity of the band at 97 cm^{-1} relative to that at 117 cm^{-1}. The small intensity changes and the overlap between these bands did not permit any conclusive quantitative measurements.

Figure 6 shows the changes described in (*i*). Quantitative measurements of the intensity ratio of the doublet, I_{331}/I_{340}, at different temperatures and at the highest and lowest pressures studied are presented in Fig. 7. The Raman spectra of the liquid and matrix isolated[7,13] Al_2Cl_6 show (Table 1) one very intense band at ~341 cm^{-1} and no indications of a doublet in this region. Further, the band at 97 cm^{-1} is less intense in both the liquid and the matrix spectrum and the weak vapour bands in the region 500–550 cm^{-1} seem to be replaced by a band of medium intensity at ~523 cm^{-1} in the matrix-isolated Al_2Cl_6 spectrum. This is also in agreement with the trends of observations (*ii*) and (*iii*). All bands found in the liquid are also present in the vapour spectrum but their relative intensities and depolarization ratios are different from those of the vapour. On going from the vapour to the liquid (Table 1) the intensity of the band at 97 cm^{-1} is decreased by 30% and the depolarization ratio is almost doubled. These changes probably indicate that the band is either a superposition of a polarized ν_4 (A_1) and a depolarized ν_{15} (B_{3g}) fundamental or is a fundamental exhibiting vibrational–rotational structure.

The Raman bands assigned as ν_1 and ν_2 in Table 1 seem to exhibit similar changes on going from the liquid or matrix isolated Al_2Cl_6 to the vapour. The intensities decrease drastically, new bands arise in the vicinity of ν_1 and ν_2 and a temperature dependence of the intensities is observed. Such changes probably indicate vibrational–rotational structure for these fundamentals. However, it is unlikely that the temperature dependence of the ν_2 doublet (Figs 6 and 7) can be accounted for in terms of vibration–rotational branches alone. Only one *Q*-branch is expected for the totally symmetric Raman band and Coriolis splitting is excluded for the A_g fundamental of a D_{2h} molecule.[20]

The 331 cm^{-1} band must be due to a Fermi resonance between $2\nu_7$ (at 334 cm^{-1} in the harmonic approximation) and ν_2 as proposed earlier.[5] In the $Al_2^{37}Cl_6$ spectrum the doublet has the same[5] or, according to our results, still smaller spacing (Table 2).

Table 2. Raman spectral data for aluminium chloride dimer (Al_2Cl_6)

$Al_2^{35}Cl_6$ (g): this work (473 K)		$\Delta\nu = \nu^{35}_{Cl} - \nu^{37}_{Cl}$ This work	$\Delta\nu = \nu^{35}_{Cl} - \nu^{37}_{Cl}$ Ref. 5 (523 K)	Assignment	
650 vw D[a]		5		$\nu_8 + \nu_{10}$	A_g
614 mw D		4.3	5.6	ν_{11}	B_{2g}
550 mw sh	P (D?)	7.5		$\nu_{13} + \nu_{18}$	B_{1g}
522 mw	P (D?)	6.5			
511 m sh	P (D?)	7.5	6.0	ν_1	A_g
342 s P		6.0	9.1	ν_2[b]	A_g
333 s P		4.8	9.2	$2\nu_7$[b]	A_g
281 w D		4.5	5.0	ν_6	B_{1g}
219 s P (+D?)		3.9	5.7	ν_3	A_g
168 w D		3.6	1.3	ν_7	B_{1g}
115 s D		2.7	1.8	ν_{12}	B_{2g}
98 s P		2.0	3.5	ν_4	A_g
50 vw D					

[a] Abbreviations: D, depolarized; P, polarized; s, strong; m, medium; w, weak; v, very; sh, shoulder.
[b] Presumably Fermi resonance; see text.

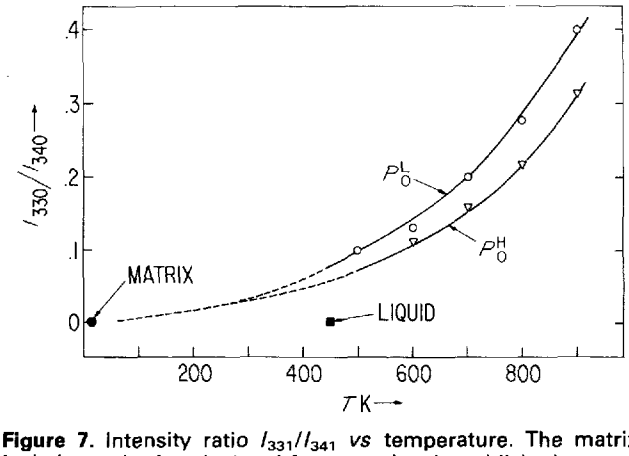

Figure 7. Intensity ratio I_{331}/I_{341} *vs* temperature. The matrix isolation point is calculated from previously published spectra (Ref. 7).

The relative Raman intensities of the doublet are inverted on going from the $Al_2^{37}Cl_6$ to the $Al_2^{35}Cl_6$ spectrum. This is clearly seen in Fig. 4 and it has been observed previously.[5] It is not understood, however, why no Fermi doublet was observed in the melt and particularly not in the matrix[7,13] in which close-lying bands should be easily resolved. Also, the molecules of Al_2Br_6 and In_2Cl_6, which are isostructural to Al_2Cl_6, do not show any splitting of their ν_1 and ν_2 fundamentals.[21]

The alternative explanation of the 331 cm^{-1} band as a hot band of the type $(\nu_2 + \nu_k - \nu_k)$ in which ν_k represents a low-frequency vibration should give a progression contrary to observation. Although the absence of this band in the matrix spectra at 20 K might indicate a hot band phenomenon, this effect does not explain the absence in the melt spectra and should not be considered seriously.

Finally, one might consider that a possible explanation for the Raman bands observed at 331 and 522 cm^{-1} and their temperature and pressure dependence could eventually indicate the existence of another undetermined vapour species of aluminium chloride in equilibrium with Al_2Cl_6 and $AlCl_3$. However, the observed relative intensity changes of these bands on isotope substitution (Fig. 4) strongly suggest that these bands are due to intramolecular properties of the same species (Al_2Cl_6) and the presence of a new species is unlikely.

Infrared spectra

Dimer. Transmission spectra of Al_2Cl_6 and $AlCl_3$ between 700 and 100 cm^{-1} are shown in Fig. 8, in which an additional emission spectrum in the same region is given. Transmission spectra in the region 75–250 cm^{-1}, showing dimer and monomer bands, are given in Fig. 9. The wavenumbers of the observed band maxima (or shoulders) for both dimer and monomer are listed in Tables 3 and 4, respectively. In addition to Al_2Cl_6 in natural abundance observed in transmission as well as in emission, Table 3 contains the wavenumbers of the $Al_2^{35}Cl_6$ bands in transmission. Finally, the shifts $\Delta\nu = \nu^{35}_{Cl} - \nu^{37}_{Cl}$ in transmission spectra and the emission spectra of Al_2Cl_6 melt[16] in natural abundance are included.

As is apparent from Fig. 8 and Table 3, the transmission and emission spectra of Al_2Cl_6 at *ca* 500 K are of comparable quality. At this temperature the blackbody emission will have a maximum at approximately 900 cm^{-1}, well suited for far-IR studies. The emissivity below 150 cm^{-1}, however, will be low, and below 200 cm^{-1} our transmission spectra had better signal-to-noise ratios than the emission spectra. Small amounts of moisture in our sample cells had to be avoided since aluminium chloride hydrolyses and forms HCl, which is immediately detectable by the intense lines of the rotational spectrum (see Fig. 9). In our experiments it was easier to avoid moisture in the emission cell with the small volume (*ca* 0.5 mm path) and saturation pressure than in the transmission cell (4 cm path) and 20–100 Torr pressure.

Our vapour spectra of the dimer agree well with the three high-frequency bands reported by Klemperer.[6] The frequency shifts between our vapour bands and the

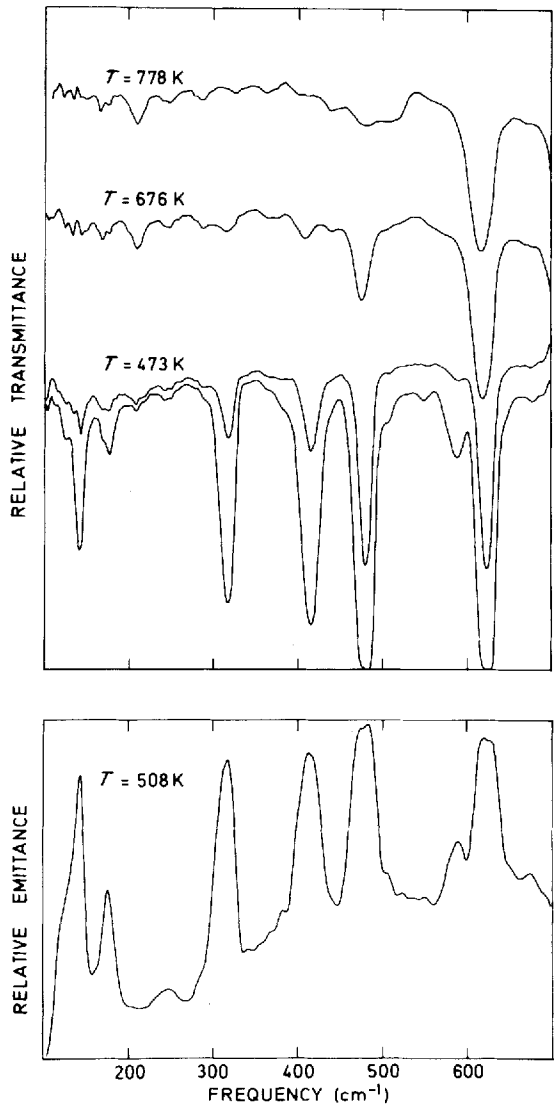

Figure 8. Infrared transmission and emission spectra of aluminium chloride dimer and monomer.

matrix isolated species in argon or nitrogen[13,22] are considerable (Table 3). Thus the importance of obtaining the real vapour spectrum is clearly demonstrated.

The accuracy of the observed isotopic dimer shifts was checked by the Teller–Redlich product rule $\pi(\lambda_i/\lambda_i^*) = |G|/|G^*|$. A reasonably good agreement is demonstrated in Table 5, considering the inherent difficulties involved in the determination of small frequency shifts in the vapour phase. These calculations support the inclusion of the observed ^{35}Cl and ^{37}Cl frequencies in the force field refinement.

Monomer. Heating the sample leads to drastic simplifications of the infrared spectra. At temperatures above 780 K only three bands remain, all of which can be attributed to fundamental frequencies of the $AlCl_3$ monomer. The bands at 616 cm^{-1} and 151 cm^{-1} agree well with earlier vapour phase data[3,6] and matrix isolation spectra.[7,22] The band at 214 cm^{-1}, assigned to the ν_2 out-of-plane bending fundamental, has not been observed in earlier spectra of the vapour phase and it differs from the corresponding band in matrix isolation spectra.[11,22] The frequency shifts for the in-plane IR

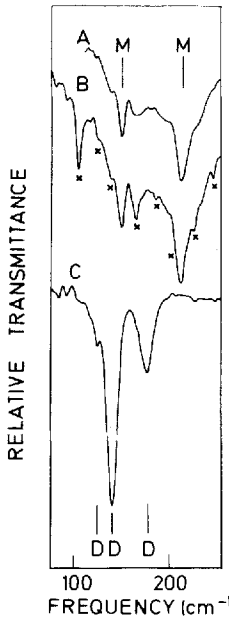

Figure 9. Infrared transmission spectra of aluminium chloride vapour: (A) $T = 843$ K; (B) $T = 843$ K [same as (A), but HCl rotational bands (×) have not been subtracted]; (C) $T = 473$ K. M and D denote monomer bands and dimer bands, respectively.

fundamentals, however, are relatively small (see Table 4).

NORMAL COORDINATE CALCULATIONS

Dimer

A normal coordinate calculation was carried out to facilitate the assignment of the low-lying fundamentals of the Al_2Cl_6 molecule. Previously, a number of calculations have been made,[4,23] but not until recently[13] have the main problems regarding the assignments been solved.

A valence force field was fitted to the observed frequencies by a standard least-squares procedure using a program originally written by Sørensen[24] and later modified in our laboratory. Although wavenumber data for both the ^{35}Cl and ^{37}Cl molecules are available, it was decided to keep the total number of unconstrained valence force constants to less than 15, i.e. the number of observed fundamental frequencies for the $Al_2^{35}Cl_6$ molecule. The notation of the applied valence coordinates is defined in Fig. 10. In addition, a torsional coordinate, τ, defined in terms of cartesian displacements of the ring atoms, $R\tau = z(A) - z(X) + z(A') - z(X')$, is introduced to describe the ring puckering vibration. A set of symmetry coordinates, including redundancies, for the bridged D_{2h} model[2] is given in Table 6.

The structural parameters (Fig. 10) from electron diffraction[2] were employed. An initial diagonal force field was transferred from Maroni *et al.*[4] and a final set of 12 valence force constants was fitted to 44 observations. Thirty observed frequencies belonged to the $Al_2^{35}Cl_6$ and $Al_2^{37}Cl_6$ molecules and 14 isotopic shifts were observed in matrix isolation spectra[13] of the mixed species (*e.g.* $Al_2^{35}Cl_n^{37}Cl_{6-n}$).

The final assignments of the fundamentals, minimizing the difference between the observed and calculated frequencies, support those of Tranquille and Fouassier.[13] The force constant pertaining to the stretching of the terminal Al—Cl bond, however, is smaller in the previous than in the present calculation owing to the introduction of a negative stretch-bend interaction.[13] This negative term improved the agreement betweeen the observed and calculated B_{1u} fundamentals.[13] In the present work it was found that the ring puckering vibration mixes with the ν_9 (B_{1u}) ($AlCl_2$ rocking mode), allowing the puckering force constant, f_τ, and an estimated value of the unobserved ν_{10} (B_{1u}) fundamental to be determined. The most recent[2] electron diffraction study of Al_2Cl_6 concludes that the puckering mode is a large amplitude vibration. Our estimated value, $\nu_{10} = 33$ cm^{-1}, based on the harmonic oscillator approach, must therefore be regarded as an approximation.

Table 3. Infrared spectral data for the aluminium chloride dimer (Al_2Cl_6)

This work				Previous work				
Natural abundance				Natural abundance				
Vapour transmission (473 K)	Vapour emission (508 K)	$Al_2^{35}Cl_6$: vapour transmission (423 K)	$Al_2^{37}Cl_6$: vapour transmission ($\Delta\nu$)[a]	Vapour (453 K)[b]	Melt emission (473 K)[c]	Matrix[d] Ar	Matrix[d] N_2	Assignment
625 s[e]	623 s	626 s	5.2	625 s	611 vs	621.5	622	ν_8 B_{1u}
590 w	590 w	591 w	4.5		578 w sh			$\nu_{12}+\nu_{16}$ B_{1u}
482 s	480 s	483 s	6.1	484 s	469 vs	485	482.5	ν_{16} B_{3u}
416 s	415 m	418 s	4.0	420 m	407 s	422	426.5	ν_{13} B_{2u}
					378 w sh			$\nu_3+\nu_9$ B_{1u}
318 s	317 m	320 s	7.5		314 s	320	322	ν_{17} B_{3u}
247 w	248 vw				246 vw			$\nu_3+\nu_{10}$ B_{1u}
176 w	177 w	178 w	5.5		176 w	174	175	ν_9 B_{1u}
142 m	140 w	143 m	3.6		139 m	143.5	143.5	ν_{18} B_{3u}
123 w sh	124 sh	123 sh	3			135	135.5	ν_{14} B_{2u}

[a] $\Delta\nu = \nu^{35}_{Cl} - \nu^{37}_{Cl}$, average values from several measurements.
[b] Ref. 6.
[c] Ref. 16.
[d] Ref. 13.
[e] Abbreviations, see Table 2.

Table 4. Infrared and Raman spectral data for the aluminium chloride monomer ($AlCl_3$)

Vapour							
This work		Previous work			Matrix isolation		
IR (843 K)	Raman (1075 K), $Al^{35}Cl_3$	IR[a] (1173 K)	Raman[b] (1093 K)	ED[c]	IR[d]	IR/Raman[e]	Interpretation
616 s[f]	~610 w	610		643 (27)	618.6 617.0 615.0 613.2 [g]	618.8 617.0 615.2 613.3 [g]	ν_3 E'
	375 s P		371 s	391 (6)		393.5 390.5 387.3 [g]	ν_1 A_1'
214 w				164 (10)	183.0		ν_2 A_2''
151 w	148 m		146 m	159 (9)	151.1	150	ν_4 E'

[a] Ref. 6.
[b] Ref. 3.
[c] Ref. 29. Frequencies calculated from electron diffraction (ED) data. Values in parentheses are estimated errors.
[d] Ref. 22.
[e] Ref. 7.
[f] Abbreviations, see Table 2.
[g] Chlorine isotope splitting.

Owing to redundancy conditions connecting the ring bending coordinates, the two bending force constants f_β and f_γ were highly correlated. Consequently, it was found that only one of the two could be determined in the least-squares refinement. As a suitable constraint, $f_\beta = f_\gamma$ was chosen.

An additional constraint was introduced by letting $f_{\alpha\theta} = f_{\theta\theta}$. The bend–bend interaction $f_{\alpha\theta}$ did not attain a stable value in the preliminary calculations and fixing its value at zero resulted in a poorer overall agreement between observed and calculated fundamental frequencies.

The two bend–bend interactions $f_{\theta\theta}$ and $f_{\theta\theta'}$ could not be determined separately unless ν_{15} (B_{3g}) was included in the set of observations. Once a value for ν_{15} is chosen, however, the inactive fundamental ν_5 (A_u) is uniquely determined since the symmetry force constant matrix of A_u, consisting of one element, equals that of B_{3g}.

Owing to a possible Fermi resonance, a mean value of 337 ± 5 cm^{-1} was chosen for ν_2 in the present calculation. In addition, a value of $\nu_{15} = 105 \pm 10$ cm^{-1} was assumed since the Raman spectra contain a broad, intense feature in the ν_4/ν_{12} region (98–115 cm^{-1}). Earlier studies[3,25] suggested that the three fundamentals ν_4, ν_{12} and ν_{15} appear in the range 89–113 cm^{-1} for the Ga_2Cl_6 molecule. Similarly, single-crystal Raman spectra of Al_2Br_6 show ν_{15} (78 cm^{-1}) to lie between ν_4 (69 cm^{-1}) and ν_{12} (85 cm^{-1}).[26] The same trend is expected for the aluminium chloride. Calculation of the statistical mechanical entropy $S^0_{298\,K}$ by insertion of the observed, calculated (ν_5, ν_{10}) and assumed (ν_{15}) fundamental frequencies into the harmonic oscillator partition function, gives $S^0_{298\,K} = 470$ J K^{-1} mol^{-1}. This agrees well with a previously reported calorimetric value[27] of $S^0_{298\,K} = 472 \pm 4$ J K^{-1} mol^{-1}.

The derived force constants are listed in Table 7 and the calculated wavenumbers for $Al_2^{35}Cl_6$ and $Al_2^{37}Cl_6$ and the mixed isotopic species are given in Table 8. It

Table 5. Teller–Redlich product rules for Al_2Cl_6

	$\pi(^{35}\lambda/^{37}\lambda)$ (obs.)	$\lvert^{35}G\rvert/\lvert^{37}G\rvert$ (calc.)
A_g	1.150	1.183
A_u		1.056
B_{1g}	1.077	1.063
B_{1u}	1.140[a]	1.129
B_{2g}	1.062	1.062
B_{2u}	1.070	1.069
B_{3g}		1.057
B_{3u}	1.129	1.130

[a] Including the calculated ν_{10} frequencies.

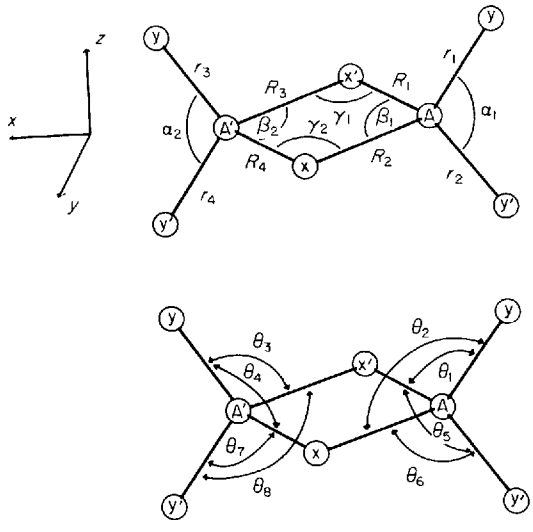

Figure 10. Valence coordinates for aluminium chloride dimer. Structural parameters used in calculations: $r = 2.065$ Å; $R = 2.252$ Å; $\alpha = 123.4°$; $\beta = 91.0°$ (Ref. 2).

Table 6. Symmetry coordinates for aluminium chloride dimer

A_g	$S_1 = \frac{1}{2}(r_1 + r_2 + r_3 + r_4)$
	$S_2 = \frac{1}{2}(R_1 + R_2 + R_3 + R_4)$
	$S_3 = 2^{-1/2}(\alpha_1 + \alpha_2)$
	$S_4 = 2^{-1/2}(\beta_1 + \beta_2)$
	$S_5 = 2^{-1/2}(\gamma_1 + \gamma_2)$
	$S_6 = 8^{-1/2}(\theta_1 + \theta_2 + \theta_3 + \theta_4 + \theta_5 + \theta_6 + \theta_7 + \theta_8)$
A_u	$S_7 = 8^{-1/2}(\theta_1 - \theta_2 - \theta_3 + \theta_4 - \theta_5 + \theta_6 + \theta_7 - \theta_8)$
B_{1g}	$S_8 = \frac{1}{2}(R_1 - R_2 - R_3 + R_4)$
	$S_9 = 8^{-1/2}(\theta_1 - \theta_2 - \theta_3 + \theta_4 + \theta_5 - \theta_6 - \theta_7 + \theta_8)$
B_{1u}	$S_{10} = \frac{1}{2}(r_1 - r_2 + r_3 - r_4)$
	$S_{11} = 8^{-1/2}(\theta_1 + \theta_2 + \theta_3 + \theta_4 - \theta_5 - \theta_6 - \theta_7 - \theta_8)$
	$S_{12} = \tau$[a]
B_{2g}	$S_{13} = \frac{1}{2}(r_1 - r_2 - r_3 + r_4)$
	$S_{14} = 8^{-1/2}(\theta_1 + \theta_2 - \theta_3 - \theta_4 - \theta_5 - \theta_6 + \theta_7 + \theta_8)$
B_{2u}	$S_{15} = \frac{1}{2}(R_1 - R_2 + R_3 - R_4)$
	$S_{16} = 2^{-1/2}(\gamma_1 - \gamma_2)$
	$S_{17} = 8^{-1/2}(\theta_1 - \theta_2 + \theta_3 - \theta_4 + \theta_5 - \theta_6 + \theta_7 - \theta_8)$
B_{3g}	$S_{18} = 8^{-1/2}(\theta_1 - \theta_2 + \theta_3 - \theta_4 - \theta_5 + \theta_6 - \theta_7 + \theta_8)$
B_{3u}	$S_{19} = \frac{1}{2}(R_1 + R_2 - R_3 - R_4)$
	$S_{20} = \frac{1}{2}(r_1 + r_2 - r_3 - r_4)$
	$S_{21} = 2^{-1/2}(\alpha_1 - \alpha_2)$
	$S_{22} = 2^{-1/2}(\beta_1 - \beta_2)$
	$S_{23} = 8^{-1/2}(\theta_1 + \theta_2 - \theta_3 - \theta_4 + \theta_5 + \theta_6 - \theta_7 - \theta_8)$

[a] For definition of the ring deformation coordinate, see text.

is apparent that the derived 12-parameter force field gives a very satisfactory agreement between the observed and calculated fundamental frequencies, including the isotopic shifts.

Table 7. Valence force field for aluminium chloride dimer (Al_2Cl_6)

Force constant	Coordinate(s) involved	Calculated value, ϕ_i	Standard error, $\sigma(\phi_i)$
Stretch and stretch–stretch		mdyn Å^{-1}	
f_r	A–Y	2.759	0.046
f_R	A–X	1.177	0.028
f_{rR}	A–Y/A–X	0.200	0.028
f_{rr}	A–Y/A–Y′	0.295	0.046
f_{RR}	A–X/A′–X	0.295	0.014
Stretch–bend		mdyn rad^{-1}	
$f_{R\theta}$	A–X/XAY	0.227	0.020
Bend and bend–bend		mdyn Å rad^{-2}	
f_α	YAY′	0.654	0.016
f_β	XAX′	0.595[a]	0.019
f_γ	AXA′		
f_θ	XAY	0.474	0.006
$f_{\alpha\theta}$	YAY′/XAY	0.165[b]	0.007
$f_{\theta\theta}$	XAY/XAY′		
$f_{\theta\theta'}$	XAY/X′AY	0.073	0.007
Ring deformation		mdyn Å rad^{-2}	
f_τ		0.323	0.044

[a] Correlated through redundancy conditions in the ring, $f_\beta = f_\gamma$ was chosen as a suitable constraint.
[b] See text.

Monomer

A force field was also developed for the $AlCl_3$ monomer. The XY_3 (D_{3h}) type molecule is a standard textbook example of normal coordinate analysis and the choice of symmetry coordinates and notation can be found elsewhere.[28]

Table 8. Observed and calculated fundamental frequencies for aluminium chloride dimer (Al_2Cl_6)

		$Al_2^{35}Cl_6$ D_{2h}		$Al_2^{37}Cl_6$ D_{2h} $\Delta\nu^b$		$Al_2^{35}Cl_5^{37}Cl$ C_{2v} $\Delta\nu^{b,c}$		$Al_2^{35}Cl_5^{37}Cl$ C_s $\Delta\nu^{b,c}$		$Al_2^{35}Cl_4^{37}Cl_2$ C_1 $\Delta\nu^{b,c}$		$Al_2^{35}Cl_4^{37}Cl_2$ D_{2h} $\Delta\nu^{b,c}$	
Fundamental	Potential energy distribution[a]	Freq. obs.	Freq. calc.	obs.	calc.	obs.	calc.	obs.	calc.	obs.	calc.	obs.	calc.
ν_1	$81r + 26R + 8\alpha$	511	510	7.5	5.4								
ν_2	$84R + 9r$	337[d]	341	6.0	8.3	2.8	2.9	0.0	0.6	2.8	3.6	5.3	5.6
ν_3	$31\beta + 31\gamma + 29\alpha + 11r$	219	219	3.9	4.5								
ν_4	$105\alpha + 43\theta + 11\beta + 11\gamma$	98	100	2.0	2.7								
ν_5	100θ		55		1.5								
ν_6	$123R + 10\theta$	281	282	4.5	4.0								
ν_7	116θ	168	168	3.6	2.8								
ν_8	$92r + 6\theta$	626	623	5.2	4.9	0.0	0.1	1.1	1.0	1.1	1.0		
ν_9	$71\theta + 20\tau + 7r$	178	178	5.5	4.5								
ν_{10}	$78\tau + 21\theta$		33		0.9								
ν_{11}	$94r + 5\theta$	614	617	4.3	5.0								
ν_{12}	$94\theta + 5r$	115	115	2.7	2.5								
ν_{13}	$97R + 15\theta + 14\gamma$	418	415	4.0	4.8	2.2	2.3	0.0	0.0	2.2	2.3	4.4	4.8
ν_{14}	97θ	123	125	3.0	2.7								
ν_{15}	100θ	105[d]	105		2.9								
ν_{16}	$94r + 15R + 7\alpha$	483	483	6.1	6.8	0.0	0.1	1.5	1.8	1.5	1.9		
ν_{17}	$60R + 16\beta + 7r$	320	318	7.5	7.2								
ν_{18}	$135\alpha + 39\theta$	143	142	3.6	3.3								

[a] $PED(I, J) = 100F(I, I)L(I, J)^2/\lambda(J)$; terms below 5 neglected.
[b] $\Delta\nu = \nu^{35}_{Cl} - \nu^{37}_{Cl}$.
[c] Ref. 13.
[d] Assumed value, see text.

Table 9. Force field for the aluminium chloride monomer ($AlCl_3$)[a]

Force constant	Calculated value	Spiridonov *et al.*[b]
Stretch and stretch–stretch		mdyn Å^{-1}
f_r	2.757 (0.063)[c]	
f_{rr}	0.065 (0.033)[d]	
F_{11}	2.888	3.20 (0.15)
F_{33}	2.692	2.88 (0.12)
Stretch–bend		mdyn rad^{-1}
F_{34}	−0.141 (0.081)[d]	−0.097 (0.012)
Bend		mdyn Å rad^{-2}
F_{44}	0.390 (0.009)	0.436 (0.038)
Out-of-plane bend		mdyn Å rad^{-2}
F_{22}	0.275 (0.005)	0.163 (0.017)

[a] The notation is that of Ref. 28. Geometrical parameters: ∠Cl–Al–Cl = 120°; r = 2.068 Å (Ref. 29).
[b] Force field estimated from electron diffraction data (Ref. 29).
[c] Values in parentheses are σ.
[d] Interaction constants highly correlated, see text.

The $AlCl_3$ force field (Table 9) was determined, using experimental $Al^{35}Cl_3$ frequencies and seven isotopic shifts from matrix isolation spectra.[7] The ν_1 (375 cm^{-1}) and ν_4 (148 cm^{-1}) values were taken from Raman spectra of the pure $Al^{35}Cl_3$ species. The differences between the ν_2 and ν_3 peaks in spectra of the pure ^{35}Cl species and $AlCl_3$ of natural isotopic abundance were estimated to be <1 cm^{-1}. Hence, the observed IR values (ν_2 = 214 cm^{-1} and ν_3 = 616 cm^{-1}) were assigned to $Al^{35}Cl_3$ in the calculations.

The calculated force field reproduces the observed frequencies with a root mean square deviation of *ca* 0.7 cm^{-1}. Although the stretch–bend interaction force constant F_{34} proved to be highly correlated to f_{rr}, it was decided not to fix its value arbitrarily. Thus a complete symmetry force field is presented.

Comparison of the monomer and dimer force fields (Tables 7 and 9) shows that the two force constants pertaining to the stretching of a monomer bond and a terminal dimer bond, are equal, *ca* 2.76 mdyn Å^{-1}. This is not surprising, as the bond lengths are identical[2,29] and a population analysis from *ab initio* calculations[30] also emphasizes the striking similarity between the two bonds.

Table 10. Calculated mean amplitudes of vibration (Å) and electron diffraction (ED) values for the aluminium chloride dimer[a]

Distance	0 K (calc.)	298 K (calc.)	420 K (calc.)	420 K ED[b])
Al···Al	0.060	0.079	0.091	0.075 (13)
Al–Cl_b	0.056	0.068	0.077	0.075 (3)
Al–Cl_t	0.044	0.048	0.053	0.049 (3)
Al···Cl_t	0.078	0.171	0.202	0.143 (34)
Cl_b···Cl_b	0.059	0.082	0.095	0.075 (13)
Cl_t···Cl_b	0.073	0.133	0.156	0.140 (9)
com Cl_t···Cl_t	0.064	0.103	0.120	0.103 (14)
trans Cl_t···Cl_t	0.076	0.139	0.164	0.169 (34)
cis Cl_t···Cl_t	0.122	0.381	0.451	0.199 (34)

[a] Values in parentheses are estimated errors ($2\sigma \times 10^3$).
[b] Ref. 2.

Table 11. Calculated mean amplitudes of vibration (Å) and electron diffraction values for the aluminium chloride monomer[a]

	Al—Cl		Cl···Cl	
T(K)	Calc.	ED	Calc.	ED
0	0.044		0.064	
298	0.048		0.100	
800	0.066	0.060 (5)[b]	0.158	0.180 (10)[b]
1150	0.078	0.074 (3)[c]	0.189	0.187 (6)[c]
1410	0.086	0.083 (2)[c]	0.209	0.198 (7)[c]

[a] Values in parentheses are estimated errors × 10^3.
[b] Ref. 1.
[c] Ref. 29.

Mean amplitudes of vibration

Calculated amplitudes for the dimer are given in Table 10 compared with the electron diffraction (ED) results of Shen.[2] The calculated values are generally higher, a fact that may indicate a lower temperature than 420 K in the experimental work. Still, the differences are within the expected uncertainty limits except for the *cis*-$Cl_t \cdots Cl_t$ and, possibly, the $Al \cdots Cl_t$ distances. These two amplitudes are strongly influenced by the f_τ force constant related to the ring puckering mode (ν_{10}). An increase in the force constant gives reduced amplitudes. Since the puckering frequency is unobserved, the f_τ value is uncertain, and more so than the standard deviation in Table 6 due to the neglect of the interaction $f_{\theta\tau}$.

Furthermore, calculations show that the amplitude of ν_{10} is exceptionally large. This was noticed by Shen, who had to treat the Al_2Cl_6 molecule as a superposition of several molecules with varying bridge bending angles.[2] Improvements both of the force field and in the interpretation of the ED data probably is possible if the ν_{10} position is found.

Vibrational amplitudes for the monomer are summarized in Table 11. The correspondence between calculated and ED values is good, particularly for the recent results of Spiridonov *et al.*[29] However, their new temperature variation technique for determination of harmonic force fields and vibrational frequencies from ED data seems to be less successful. For example, the out-of-plane bending mode ν_2, calculated to 164(10) cm^{-1},[29] is far from the 214 cm^{-1} (Table 4) observed in IR.

Acknowledgements

The authors are grateful to C. J. Nielsen and J. Hvistendahl for valuable help with the infrared recordings. A postdoctoral fellowship to T.T. from NTNF and financial support from NAVF are acknowledged.

REFERENCES

1. E. Z. Zasorin and N. G. Rambidi, *Zh. Strukt. Khim.* **8**, 391 (1967).
2. Q. Shen, PhD Thesis, Oregon State Univ. (1974).
3. I. R. Beattie and J. R. Horder, *J. Chem. Soc. A* 2655 (1969).
4. V. A. Maroni, D. M. Gruen, R. L. McBeth and E. J. Cairns, *Spectrochim. Acta, Part A* **26**, 418 (1970).
5. C. Rohrbasser, Thesis, Fribourg, Switzerland (1976).
6. W. Klemperer, *J. Chem. Phys.* **24**, 353 (1956).
7. I. R. Beattie, H. E. Blayden, S. M. Hall, S. N. Jenny and J. S. Ogden, *J. Chem. Soc., Dalton Trans.* 666 (1976).
8. H. Gerding and E. Smit, *Z. Phys. Chem. Abt. B* **50**, 171 (1941).
9. E. V. Pershina and S. S. Raskin, *Opt. Spectrosc.* **13**, 272 (1962).
10. H. A. Øye, E. Rytter, P. Klaeboe and S. J. Cyvin, *Acta Chem. Scand.* **25**, 559 (1971).
11. M. L. Lesiecki and J. S. Shirk, *J. Chem. Phys.* **56**, 4171 (1972).
12. V. H. Schnöckel, *Z. Anorg. Allg. Chem.* **424**, 203 (1976).
13. M. Tranquille and M. Fouassier, *J. Chem. Soc., Faraday Trans. II* **76**, 26 (1980).
14. E. Rytter, J. Hvistendahl and T. Tomita, *J. Mol. Struct.* **79**, 323 (1982).
15. P. Klaeboe, E. Rytter, C. E. Sjøgren and T. Tomita, *SPIE J.* **289**, 283 (1981).
16. J. Hvistendahl, P. Klaeboe, E. Rytter and H. A. Øye, *Inorg. Chem.*, submitted.
17. T. Tomita and E. Rytter, *Yoyuen (Japan)* **24**, 32 (1981).
18. G. N. Papatheodorou, in *Argonne National Laboratory Report*, ANL-75-45 (1975).
19. G. N. Papatheodorou and S. A. Solin, *Phys. Rev. B* **13**, 1471 (1976).
20. G. Herzberg, *Molecular Spectra and Molecular Structure*, Vol. II, p. 491, Van Nostrand, New York (1945).
21. M. A. Capote and G. N. Papatheodorou, to be published.
22. R. G. S. Pong, A. E. Shirk and J. S. Shirk, *Ber. Bunsenges. Phys. Chem.* **82**, 79 (1978).
23. R. P. Bell and H. C. Longuet-Higgins, *Proc. Roy. Soc. London, Ser. A* **183**, 357 (1945).
24. S. Bjørklund, E. Augdahl, D. H. Christensen and G. O. Sørensen, *Spectrochim. Acta, Part A* **32**, 1021 (1976).
25. I. R. Beattie, T. Gilson, G. A. Ozin, *J. Chem. Soc. A* 813 (1968).
26. I. R. Beattie and T. R. Gilson, *Proc. Roy. Soc. London, Ser. A* **307**, 407 (1968).
27. L. D. Polyachenok, G. D. Dudchik and O. G. Polyachenok, *Russ. J. Phys. Chem.* **50**, 227 (1976).
28. J. A. Ladd, W. J. Orville-Thomas and B. C. Cox, *Spectrochim. Acta* **19**, 1911 (1963).
29. V. P. Spiridonov, A. G. Gershikov, E. Z. Zasorin, N. I. Popenko, A. A. Ivanov and L. I. Ermolayeva, *High Temp. Sci.* **14**, 285 (1981).
30. M. F. Lappert, J. B. Pedley, G. J. Sharp and M. F. Guest, *J. Chem. Soc., Faraday Trans. II* **72**, 539 (1976).

Received 25 April 1983